

On-the-Fly Joint Feature Selection and Classification

Yasitha Warahena Liyanage, *Student member, IEEE*, Daphney–Stavroula Zois, *Member, IEEE*, and Charalampos Chelmiss, *Member, IEEE*

Abstract—Joint feature selection and classification in an online setting is essential for time-sensitive decision making. However, most existing methods treat this coupled problem independently. Specifically, online feature selection methods can handle either streaming features or data instances offline to produce a fixed set of features for classification, while online classification methods classify incoming instances using full knowledge about the feature space. Nevertheless, all existing methods utilize a set of features, common for all data instances, for classification. Instead, we propose a framework to perform joint feature selection and classification on-the-fly, so as to minimize the number of features evaluated for every data instance and maximize classification accuracy. We derive the optimum solution of the associated optimization problem and analyze its structure. Two algorithms are proposed, ETANA and F-ETANA, which are based on the optimum solution and its properties. We evaluate the performance of the proposed algorithms on several public datasets, demonstrating (i) the dominance of the proposed algorithms over the state-of-the-art, and (ii) its applicability to broad range of application domains including clinical research and natural language processing.

Index Terms—large-scale data mining, big data analytics, feature selection, classification.

1 INTRODUCTION

FEATURE selection is the process of selecting a subset of the most informative features from a large set of potentially redundant features with the objective of maximizing classification accuracy, alleviating the effect of the curse of dimensionality, speeding up the training process and improving interpretability [1], [2].

Most existing work on feature selection [3], [4], [5], [6], [7], [8], [9], [10], [11], [12], [13], [14], [15], [16], [17], [18], [19], [19], [20] extracts a subset of discriminative features that can globally describe the data well, where the same feature subset is used to classify all instances during classification (see Fig. 1(a)). Only a handful of feature selection methods have considered the feature evaluation cost and costs associated with misclassification, which play a key role in many real-world applications [21], [22]. On the other hand, existing online classification techniques [23], [24], [25], [26], [27], [28], [29], [30], [31], [32], [33] update model parameters by examining incoming data instances one at a time; such methods are not only affected by noisy and missing data, but also face scalability constraints [33].

In a depart from existing feature selection and classification methods, we study the problem of on-the-fly joint feature selection and classification (OJFC) in an online setting. Specifically, the goal of OJFC is to minimize the number of feature evaluations for classification individually for each instance, while achieving high classification accuracy across all instances. This is particularly important and necessary for real-world applications requiring time-sensitive deci-

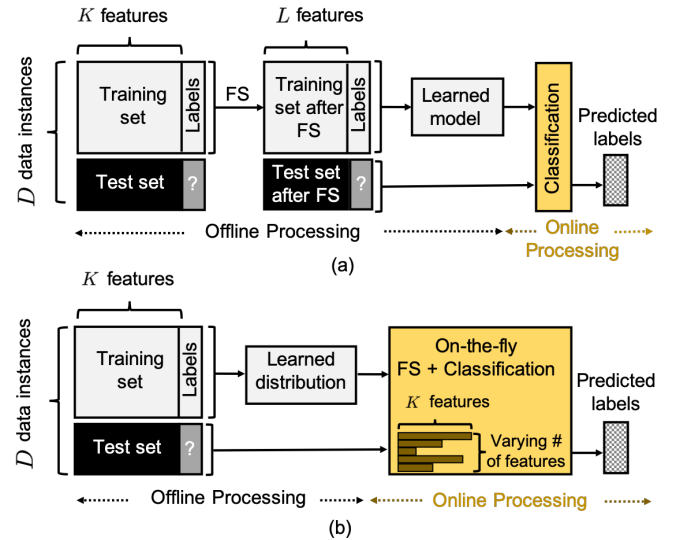


Fig. 1: Using a $K \times D$ matrix, (a) existing feature selection (FS) methods extract a set $L \ll K$ of features, which is common for all data instances during classification. In contrast, (b) the proposed on-the-fly joint feature selection and classification approach utilizes a varying number of features to classify each data instance online using a model learned offline from all features.

sions such as weather forecasting [34], transportation [35], stock markets prediction [36], clinical research [37], and natural disasters prediction [38]. Therefore, the proposed method utilizes a varying number of features to classify each data instance (see Fig. 1(b)).

To address the challenges associated with the problem of OJFC, we define an optimization problem which simultane-

- Y. Warahena Liyanage and D.-S. Zois are with the Department of Electrical and Computer Engineering, University at Albany, SUNY, NY, 12222.
E-mail: yliyanage@albany.edu, dzois@albany.edu
- C. Chelmiss is with the Department of Computer Science, University at Albany, SUNY, NY, 12222.
E-mail: cchelmiss@albany.edu

ously minimizes the number of features evaluated and maximizes classification accuracy. The solution to this optimization problem leads to an approach that sequentially reviews features and classifies a data instance once it determines that including additional features cannot further improve the quality of classification. However, the computational complexity of the optimum solution increases exponentially with the number of classes in multi-class classification tasks. To improve the scalability of our approach, we propose an efficient implementation, which exploits the structure of the optimum solution. Specifically, the functions related to the optimum solution are shown to be concave, continuous and piecewise linear on the domain of a sufficient statistic. As a result, the optimum solution exhibits a threshold structure to decide between continuing the feature evaluation process and stopping. A stochastic gradient algorithm is utilized to estimate the optimal linear thresholds. Extensive experimental evaluation using seven publicly available datasets shows the superiority of the proposed approach in terms of classification accuracy, average number of features used per data instance, and time required for joint feature selection and classification compared to the state-of-the-art. Further, our evaluation results indicate that the proposed efficient implementation drastically reduces training time without a drop in accuracy as compared to the optimum solution. All proofs are included in Appendices A and B.

2 RELATED WORK

In this section, we summarize the most relevant prior work on (i) online feature selection and (ii) online classification techniques.

2.1 Online feature selection

In contrast to offline feature selection methods that are designed for static datasets with fixed number of features and data samples, online feature selection methods are capable of handling either streaming features or streaming data samples to choose a subset of features from a larger set of potentially redundant features [14], [19], [20]. Online feature selection methods can be generally grouped into two groups:

(a) Streaming Features: In this branch of online feature selection problems, the number of data instances is considered constant while features arrive one at a time [3], [4], [5], [6], [7], [8], [9], [10]. In [3], a newly arriving feature is selected if the improvement in the model is greater than a predefined threshold. [5], [6] try to extract features in the Markov blanket of the class variable using a forward algorithm, where thresholds on probability approximations to measure conditional independence (e.g. G^2 -test [5], Fisher’s Z -test [6]) are employed. Such threshold-based methods [3], [4], [5], [6] require prior information about the feature space [7]. Recently, rough set theory based methods [7], [8], [9], [10] have been explored. Such methods do not require any domain knowledge [8]. However, methods proposed in [8], [10] are not applicable to numerical features, while methods [7], [9] are much slower in feature selection compared to the state-of-the-art streaming feature selection methods.

(b) Streaming Data: In this problem setting, the number of

features is considered constant, while data instances arrive over time [11], [12], [13]. Such methods [11], [12], [13], are limited to binary classification and/or impose hard constraints on the number of non-zero elements in the model, requiring the user to define the number of features that need to be selected *a priori* [33].

2.2 Online Classification

Online classification methods, also referred to as online learning, use sequentially arriving data to update the function of a classifier. This is in contrast to batch learning techniques where a collection of training data is used to train a classifier offline, without further updates once training is complete [33]. Most widely used online learning methods [23], [24], [25] are either limited to binary classification [23], [24] or require solving a complex optimization problem at each iteration, and require prior information to tune parameters in the model [25]. On the other hand, traditional gradient based methods [26], [27], [28], [29] not only require to compute the gradient of a cost function, but also require to solve an optimization problem at each iteration. Cost-sensitive extensions of traditional online classification methods, which account for misclassification costs have been recently explored [25], [30], [31], [32]. Unlike our approach, [25], [30] do not optimize the misclassification cost directly [33], while [30], [31], [32] are limited to binary classification. Last but not least, most existing methods are highly susceptible to noise and/or incomplete data [33].

3 ON-THE-FLY JOINT FEATURE SELECTION AND CLASSIFICATION

Consider a set S of data instances, with each data instance $s \in S$ being described using an assignment of values $f = \{f_1, f_2, \dots, f_K\}$ to a set $F = \{F_1, F_2, \dots, F_K\}$ of K features. Each data instance s is drawn from some probability distribution over the feature space such that for each assignment f to F , we have a probability $P(F = f)$. Further, each instance s may belong to one of N classes, with corresponding *a priori* probability $P(T = T_i) = p_i$ for each assignment $T_i, i = 1, 2, \dots, N$, of the class variable T . Moreover, coefficients $c_k > 0, k = 1, 2, \dots, K$, represent the cost of evaluating features F_k , respectively, and coefficients $M_{i,j} \geq 0, i, j \in \{1, \dots, N\}$, denote the misclassification cost of selecting class T_j when class T_i is true.

To select one out of N possible classes for each data instance s , our proposed approach evaluates features sequentially, where at each step it has to decide between stopping and continuing the feature evaluation process based on the accumulated information thus far and the cost of evaluating the remaining features. Herein, we introduce a pair of random variables (R, D_R) , where $0 \leq R \leq K$ (referred to as *stopping time* [39] in decision theory) denotes the feature at which the framework assigns s to a specific class, and $D_R \in \{1, \dots, N\}$, which depends on R , denotes the possibility to select among the N classes. The event $\{R = k\}$ depends only on the feature set $\{F_1, F_2, \dots, F_k\}$, whereas the event $\{D_R = j\}$ represents choosing class T_j based on information accumulated up to feature R . The

goal is to select random variables R and D_R by solving the following optimization problem:

$$\underset{R, D_R}{\text{minimize}} J(R, D_R), \quad (1)$$

where the cost function is defined as:

$$J(R, D_R) \triangleq \mathbb{E} \left\{ \sum_{k=1}^R c_k \right\} + \sum_{j=1}^N \sum_{i=1}^N M_{ij} P(D_R = j, T = T_i), \quad (2)$$

in which the first term denotes the cost of evaluating features, and the second term penalizes misclassification errors.

To solve the optimization problem defined in Eq. (1), we define a sufficient statistic of accumulated information, the *a posteriori* probability vector π_k , as follows:

$$\pi_k \triangleq [\pi_k^1, \pi_k^2, \dots, \pi_k^N]^T, \quad (3)$$

where the k th feature is evaluated to generate outcome f_k , and $\pi_k^i \triangleq P(T_i | F_1, \dots, F_k)$. To simplify the notation, $P(T_i | F_1, \dots, F_k)$ is used in lieu of $P(T = T_i | F_1 = f_1, \dots, F_k = f_k)$ subsequently. Assuming that features in set F are independent given the class variable T^1 , π_k can be computed recursively as in Lemma 1.

Lemma 1. *The a posteriori probability vector $\pi_k \in [0, 1]^N$ can be recursively computed as:*

$$\pi_k = \frac{\text{diag}(\Delta_k(F_k))\pi_{k-1}}{\Delta_k^T(F_k)\pi_{k-1}}, \quad (4)$$

where $\Delta_k(F_k) \triangleq [P(F_k | T_1), P(F_k | T_2), \dots, P(F_k | T_N)]^T$, $\text{diag}(A)$ denotes a diagonal matrix with diagonal elements being the elements in vector A , and $\pi_0 \triangleq [p_1, p_2, \dots, p_N]^T$.

Next, we simplify the probability $P(D_R = j, T = T_i)$ exploiting the definition of the *a posteriori* probability π_k^i .

Lemma 2. *Based on the fact that $x_R = \sum_{k=0}^K x_k \mathbb{1}_{\{R=k\}}$ for any sequence of random variables $\{x_k\}$, where $\mathbb{1}_A$ is the indicator function for event A (i.e., $\mathbb{1}_A = 1$ when A occurs, and $\mathbb{1}_A = 0$ otherwise), the probability $P(D_R = j, T_i)$ can be written as follows:*

$$P(D_R = j, T_i) = \mathbb{E} \left\{ \pi_R^i \mathbb{1}_{\{D_R=j\}} \right\}. \quad (5)$$

Using Lemma 2, the average cost in Eq. (2) can be written compactly as:

$$J(R, D_R) = \mathbb{E} \left\{ \sum_{k=1}^R c_k + \sum_{j=1}^N \left(\sum_{i=1}^N M_{ij} \pi_R^i \right) \mathbb{1}_{\{D_R=j\}} \right\}, \quad (6)$$

which in turn can be rewritten as follows:

$$J(R, D_R) = \mathbb{E} \left\{ \sum_{k=1}^R c_k + \sum_{j=1}^N M_j^T \pi_R \mathbb{1}_{\{D_R=j\}} \right\}, \quad (7)$$

where $M_j \triangleq [M_{1,j}, M_{2,j}, \dots, M_{N,j}]$.

To obtain the optimum stopping time R , we must first obtain the optimum decision rule D_R for any given R . In the process of finding the optimum decision rule, we need to find a lower bound (independent of D_R) for the second term inside the expectation in Eq. (7), which is the part of the equation that depends on D_R . Theorem 1 provides such bound.

Theorem 1. *For any classification rule D_R given stopping time R , $\sum_{j=1}^N M_j^T \pi_R \mathbb{1}_{\{D_R=j\}} \geq g(\pi_R)$, where $g(\pi_R) \triangleq \min_{1 \leq j \leq N} [M_j^T \pi_R]$. The optimum rule is defined as follows:*

$$D_R^{\text{optimum}} = \arg \min_{1 \leq j \leq N} [M_j^T \pi_R]. \quad (8)$$

From Theorem 1, we conclude that:

$$J(R, D_R) \geq J(R, D_R^{\text{optimum}}), \text{ where} \\ J(R, D_R^{\text{optimum}}) = \min_{D_R} J(R, D_R). \quad (9)$$

Thus, we can reduce the cost function in Eq. (7) to one which depends only on the stopping time R as follows:

$$\tilde{J}(R) = \mathbb{E} \left\{ \sum_{k=1}^R c_k + g(\pi_R) \right\}. \quad (10)$$

To optimize the cost function in Eq. (10) with respect to R , we need to solve the following optimization problem:

$$\min_{R \geq 0} \tilde{J}(R) = \min_{R \geq 0} \mathbb{E} \left\{ \sum_{k=1}^R c_k + g(\pi_R) \right\}. \quad (11)$$

Since $R \in \{0, 1, \dots, K\}$, the optimum strategy consists of a maximum of $K + 1$ stages, where the optimum solution must minimize the corresponding average cost going from stages 0 to K . The solution can be obtained using *dynamic programming* [40].

Theorem 2. *For $k = K - 1, \dots, 0$, function $\bar{J}_k(\pi_k)$ is related to $\bar{J}_{k+1}(\pi_{k+1})$ through the equation:*

$$\bar{J}_k(\pi_k) = \min \left[g(\pi_k), c_{k+1} + \sum_{F_{k+1}} \Delta_{k+1}^T(F_{k+1})\pi_k \right. \\ \left. \times \bar{J}_{k+1} \left(\frac{\text{diag}(\Delta_{k+1}(F_{k+1}))\pi_k}{\Delta_{k+1}^T(F_{k+1})\pi_k} \right) \right], \quad (12)$$

where $\bar{J}_K(\pi_K) = g(\pi_K)$.

The optimum stopping strategy derived from Eq. (12) has a very intuitive structure. Specifically, it stops at stage k , where the cost of stopping (the first expression in the minimization) is no greater than the expected cost of continuing given all information accumulated at the current stage k (the second expression in the minimization). Equivalently, at each stage k , our method faces two options given π_k : (i) stop evaluating features and select optimally between the N classes, or (ii) continue with the next feature. The cost of stopping is $g(\pi_k)$, whereas the cost of continuing is $c_{k+1} + \sum_{F_{k+1}} \Delta_{k+1}^T(F_{k+1})\pi_k \times \bar{J}_{k+1} \left(\frac{\text{diag}(\Delta_{k+1}(F_{k+1}))\pi_k}{\Delta_{k+1}^T(F_{k+1})\pi_k} \right)$.

Based on Lemma 1, and Theorems 1 and 2, we present **ETANA**, an on-the-fly feature selection and classification Algorithm. Initially, the posterior probability vector π_0 is set to $[p_1, p_2, \dots, p_N]$, and the two terms in Eq. (12) are compared. If the first term is less than or equal to the second term, ETANA classifies the instance under examination to the appropriate class, based on the optimum rule in Eq. (8). Otherwise, the first feature is evaluated. ETANA repeats these steps until either it decides to classify the instance using $< K$ features, or using all K features.

To implement ETANA, we first need to solve the *dynamic programming* recursion in Eq. (12). This can be achieved by quantizing the interval $[0, 1]$ over N values such that

1. Even though validation of this assumption is beyond the scope of this paper, we find our proposed method to work well in practice.

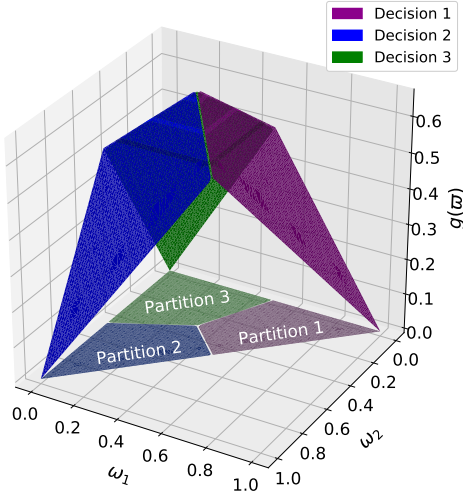


Fig. 2: Illustration of Lemma 3 when the number N of classes equals to 3, with misclassification costs $M_1 = [0, 1, 1]$, $M_2 = [1, 0, 1]$ and $M_3 = [1, 1, 0]$.

$\sum_{i=1}^N \pi_k^i = 1$ to generate different possible vectors π_k . We can then compute a $(K+1) \times d$ matrix, where each row contains values of the function $\bar{J}_k(\pi_k)$, $k = 0, 1, \dots, K$, evaluated using Theorem 2 for all possible d vectors of π_k . Although this computation requires only *a priori* information, the size of this matrix (i.e., d) grows exponentially with the number N of classes, resulting in a computationally expensive solution. To address this challenge, we propose an efficient implementation of ETANA in Section 4.

4 EFFICIENT IMPLEMENTATION OF ETANA

In this section, we present a fast version of ETANA, namely, **F-ETANA**, that exploits structural properties of the optimum classification rule in Eq. (8) and the optimum stopping strategy in Eq. (12).

Consider a general form of the function $g(\pi_R)$ used to derive the optimum classification rule in Eq. (8) as follows:

$$g(\varpi) \triangleq \min_{1 \leq j \leq N} [M_j^T \varpi], \varpi \in [0, 1]^N, \quad (13)$$

where $\varpi = [\omega_1, \dots, \omega_N]^T$, such that $\omega_i \geq 0$, $\sum_{i=1}^N \omega_i = 1$. Here, the domain of $g(\varpi)$ is the probability space of ϖ , which is a $N-1$ dimensional unit simplex. Function $g(\varpi)$ has some interesting properties as described in Lemma 3.

Lemma 3. *Function $g(\varpi)$ is concave, continuous, and piecewise linear and consist of at most N hyperplanes.*

Fig. 2 shows a visualization of Lemma 3, when $N = 3$, so that the domain of $g(\varpi)$ is a 2-dimensional unit simplex (i.e., an equilateral triangle). Next, we consider the general form of the optimum stopping strategy in Eq. (12) as follows:

$$\bar{J}_k(\varpi) = \min \left[g(\varpi), c_{k+1} + \sum_{F_{k+1}} \Delta_{k+1}^T(F_{k+1}) \varpi \times \bar{J}_{k+1} \left(\frac{\text{diag}(\Delta_{k+1}(F_{k+1})) \varpi}{\Delta_{k+1}^T(F_{k+1}) \varpi} \right) \right]. \quad (14)$$

Lemma 4 summarizes the key properties enjoyed by this function.

Lemma 4. *The functions $\bar{J}_k(\varpi)$, $k = 0, \dots, K-1$, are concave, continuous, and piecewise linear.*

The fact that $g(\varpi)$ and $\bar{J}_k(\varpi)$ are concave and piecewise linear allows for a compact representation of these functions. Recall that according to Theorem 2, we stop at stage k whenever $g(\varpi) \leq \bar{C}_{k+1}(\varpi)$, where $\bar{C}_{k+1}(\varpi)$ is the optimum cost-to-go at stage k given by $c_{k+1} + \sum_{F_{k+1}} \Delta_{k+1}^T(F_{k+1}) \varpi \times \bar{J}_{k+1} \left(\frac{\text{diag}(\Delta_{k+1}(F_{k+1})) \varpi}{\Delta_{k+1}^T(F_{k+1}) \varpi} \right)$. In particular, to decide between continuing and stopping, it is sufficient to keep track of the thresholds at the intersections of $g(\varpi)$ with every $\bar{C}_{k+1}(\varpi)$ as stated in Theorem 3 below.

Theorem 3. *At every stage k , there exists at most N threshold curves that separate the unit simplex into regions which alternatively switch between continuation to the next stage and stopping. In particular, the region starting from every corner of the $N-1$ dimensional unit simplex always corresponds to stopping the feature evaluation process.*

Theorem 3 turns out to be very important. Specifically, the region where the *a posteriori* probability vector π_R falls into will help decide between continuing to the next stage or stopping. This provides an alternative fast implementation of the optimum solution using thresholds. Fig. 3 shows a visualization of Theorem 3; both sub-figures contain maximum number of threshold curves (i.e., 3 since $N = 3$).

4.1 Stochastic Gradient Algorithm for Estimating Optimum Linear Thresholds

We propose a stochastic gradient algorithm to estimate the threshold curves described in Theorem 3. For ease of implementation, we restrict the approximation to linear threshold curves of the form given in Eq. (15).

Let $\theta_{\bar{D}_{\bar{R}}} \triangleq [\theta_{\bar{D}_{\bar{R}}}^1, \theta_{\bar{D}_{\bar{R}}}^2, \dots, \theta_{\bar{D}_{\bar{R}}}^N]$ denote the parameters of a linear hyperplane, where \bar{R} is the number of features evaluated so far, and $\bar{D}_{\bar{R}} = j$, $\bar{R} \in \{0, 1, \dots, K\}$, $j \in \{1, \dots, N\}$ represents a decision choice. Then, the decision Z_θ to “stop” or “continue” at each stage \bar{R} under the decision choice $\bar{D}_{\bar{R}} = j$, as function of ϖ , is defined as follows:

$$Z_{\theta_{\bar{D}_{\bar{R}}}}(\varpi) = \begin{cases} \text{stop,} & \text{if } \theta_{\bar{D}_{\bar{R}}}^T \varpi \leq 0 \\ \text{continue,} & \text{otherwise} \end{cases}. \quad (15)$$

Decision $Z_{\theta_{\bar{D}_{\bar{R}}}}$ is indexed by $\theta_{\bar{D}_{\bar{R}}}$ to show the explicit dependency of the parameters on the decision, where $\theta_{\bar{D}_{\bar{R}}} \triangleq [\theta_{\bar{D}_{\bar{R}}^0}, \theta_{\bar{D}_{\bar{R}}^1}, \dots, \theta_{\bar{D}_{\bar{R}}^{K-1}}] \in \mathbb{R}^{K \times N}$, $\bar{D}_{\bar{R}} = j$, $\forall \bar{R}$, is the concatenation of $\theta_{\bar{D}_{\bar{R}}}$ vectors, one for each stage \bar{R} . Now, recall the cost function in Eq. (10). Since we are interested in finding linear thresholds for each decision choice $\bar{D}_{\bar{R}} = j$ independently, we use a modified version of the cost function in Eq. (10) as follows:

$$\tilde{H}(\theta_{\bar{D}_{\bar{R}}}) = \mathbb{E}_{Z_{\theta_{\bar{D}_{\bar{R}}}}} \left\{ \sum_{k=1}^{\bar{R}} c_k + M_{\bar{D}_{\bar{R}}} \pi_{\bar{R}} \right\}. \quad (16)$$

Algorithm 1 generates a sequence of estimates $\theta_{\bar{D}_{\bar{R}},t}$ by computing the gradient $\nabla_{\theta_{\bar{D}_{\bar{R}}}} \tilde{H}(\theta)$. Here, $\theta_{\bar{D}_{\bar{R}},t}$ denotes the

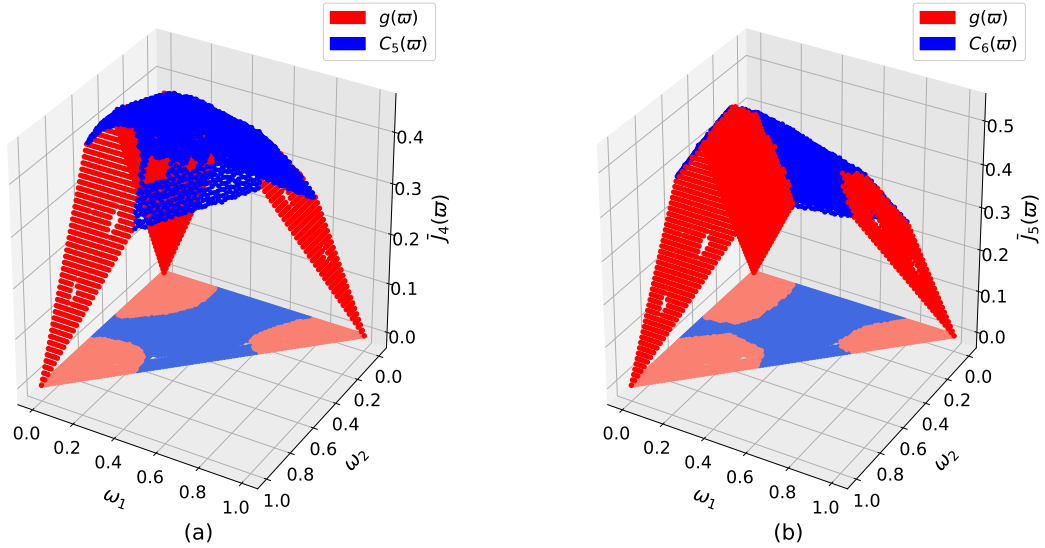


Fig. 3: Illustration of Theorem 3 (better seen in color): (a) at stage 4 and (b) at stage 5, using MLL dataset with misclassification costs $M_1 = [0, 1, 1]$, $M_2 = [1, 0, 1]$ and $M_3 = [1, 1, 0]$. The MLL dataset contains 72 samples, each of which comprises 5848 gene expression values belonging to one of 3 diagnostic classes [41]. In both cases, the blue region corresponds to continuation to the next stage, while the red region corresponds to stopping.

Algorithm 1 Stochastic Gradient Algorithm for Estimating Optimal Linear Thresholds

Require: Initial parameters $\theta_{\bar{D},0}$

Output: Optimal parameters $\theta_{\bar{D},opt}$

- 1: **for** iterations $t = 0, 1, 2, \dots$ **do**
 - 2: Evaluate $\tilde{H}(\theta_{\bar{D},t} + \beta_t \alpha_t)$ and $\tilde{H}(\theta_{\bar{D},t} - \beta_t \alpha_t)$ using Function 2 based on Eq. (16)
 - 3: Estimate $\hat{\nabla}_{\theta_{\bar{D}}} \tilde{H}(\theta_{\bar{D},t})$ using Eq. (17)
 - 4: Update $\theta_{\bar{D},t}$ to $\theta_{\bar{D},t+1}$ using Eq. (18)
 - 5: Stop if $\|\hat{\nabla}_{\theta_{\bar{D}}} \tilde{H}(\theta_{\bar{D},t})\|_2 \leq \varepsilon$ or maximum number t_{max} of iterations reached
 - 6: **end for**
 - 7: **return** $\theta_{\bar{D},opt}$
-

estimate of $\theta_{\bar{D}}$ at iteration t . Although evaluating the gradient in closed form is intractable due to the non-linear dependency of $\tilde{H}(\theta_{\bar{D}})$ and $\theta_{\bar{D}}$, estimate $\hat{\nabla}_{\theta_{\bar{D}}} \tilde{H}(\theta_{\bar{D}})$ can be computed using a simulation-based gradient estimator. For simplicity, we opted for the SPSA algorithm [42], among the several simulation-based gradient estimators in the literature [43]. SPSA algorithm estimates the gradient at each iteration t using a finite difference method and a random direction α_t , as follows:

$$\hat{\nabla}_{\theta_{\bar{D}}} \tilde{H}(\theta_{\bar{D},t}) = \frac{\tilde{H}(\theta_{\bar{D},t} + \beta_t \alpha_t) - \tilde{H}(\theta_{\bar{D},t} - \beta_t \alpha_t)}{2\beta_t} \alpha_t, \quad (17)$$

where $\alpha_t^i = \begin{cases} -1, & \text{with probability } 0.5 \\ +1, & \text{with probability } 0.5 \end{cases}$.

Using the gradient estimate in Eq. (17), parameter $\theta_{\bar{D},t}$ is updated as follows:

$$\theta_{\bar{D},t+1} = \theta_{\bar{D},t} - a_t \hat{\nabla}_{\theta_{\bar{D}}} \tilde{H}(\theta_{\bar{D},t}), \quad (18)$$

where a_t and β_t are typically chosen as in [42]:

$$\begin{aligned} a_t &= \varepsilon(t+1+\varsigma)^{-\kappa}, & 0.5 < \kappa \leq 1, & \quad \varepsilon, \varsigma > 0, \\ \beta_t &= \mu(t+1)^{-\nu}, & 0.5 < \nu \leq 1, & \quad \mu > 0. \end{aligned} \quad (19)$$

Algorithm 1 is guaranteed to converge to a local minimum with probability one [42]. We consider the following stopping criteria: $\|\hat{\nabla}_{\theta_{\bar{D}}} \tilde{H}(\theta_{\bar{D},t})\|_2 \leq \varepsilon$, or algorithm stops when it reaches a user-defined maximum number of iterations. Finally, $\tilde{H}(\cdot)$ in Eq. (16) is estimated using Function 2.

Function 2 $\tilde{H}(\cdot)$

Require: parameter $\theta_{\bar{D}}$ and π_0

Output: $\tilde{H}(\theta_{\bar{D}})$

Initialization : $k = 0$ and $\tilde{H} = 0$

- 1: **while** $\theta_{\bar{D}_k}^T \pi_k \geq 0$ **do**
 - 2: $k = k + 1$
 - 3: Obtain a new feature F_k
 - 4: Update π_k using Eq. (4)
 - 5: $\tilde{H} = \tilde{H} + c_k$
 - 6: **end while**
 - 7: $\tilde{H} = \tilde{H} + M_{\bar{D}_k}^T \pi_k$
 - 8: **return** \tilde{H}
-

5 EXPERIMENTAL RESULTS

In this section, we conduct an extensive set of experiments to evaluate the performance of ETANA and F-ETANA using seven benchmark datasets: 4 DNA Microarray Datasets (Lung Cancer, Lung2, MLL, Car) [41], 2 NIPS 2003 feature selection challenge datasets (Dexter, Madelon) [44], and 1 high dimensional dataset (News20) [45]. Table 1 summarises these datasets. For Madelon, Dexter and MLL datasets, we use the originally provided training and validation sets,

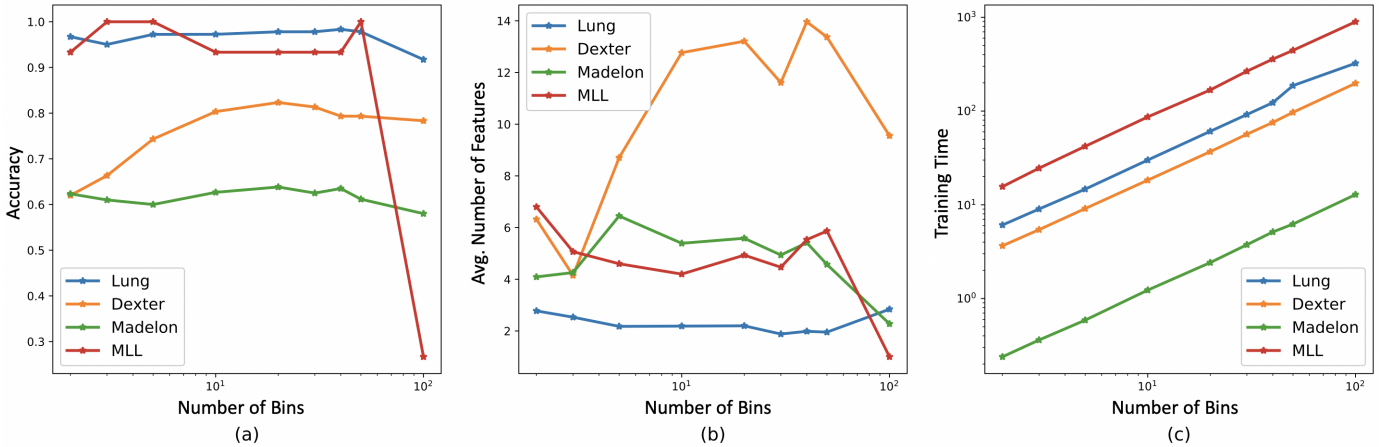


Fig. 4: Variation of (a) accuracy, (b) average number of features, and (c) training time (sec) as a function of the number $V \in \{2, 3, 5, 10, 20, 30, 40, 50, 100\}$ of bins using Lung Cancer, Dexter, Madelon and MLL datasets.

TABLE 1: Datasets used in our experiments.

Dataset	# Instances	# Features	# classes
Madelon	2,000	500	2
Lung	181	12,533	2
MLL	72	5,848	3
Dexter	300	20,000	2
Car	174	9,182	11
Lung2	203	3,312	5
News20	19,996	1,355,191	2

while for Lung Cancer, Lung2 and Car datasets, we report five-fold cross validated results. All experiments are conducted on a PC with Intel(R) Core(TM) i7-7700 @3.60 GHz CPU with 16 GB memory, running Windows 10 Pro, 64 bit operating system.

5.1 Practical Considerations

Here, we discuss some practical considerations. We use a smoothed maximum likelihood estimator to estimate $p(F_k|T_i)$, $k = 1, \dots, K$, $i = 1, \dots, N$, after quantizing the feature space. Specifically, $\hat{p}(F_k|T_i) = \frac{S_{k,i+1}}{S_i+V}$, where $S_{k,i}$ denotes the number of samples that satisfy $F_k = f_k$ and belong to class T_i , S_i denotes the total number of samples belonging to class T_i , and V is the number of bins considered. The effect of the number V of bins on the performance of our algorithm is studied in Section 5.2. We estimate the *a priori* probabilities as $P(T_i) = \frac{S_i}{\sum_{i=1}^N S_i}$, $i = 1, \dots, N$.

Feature ordering is crucial for early stopping. Different features can hinder or facilitate the quick identification of the class of which an instance may belong to. Consider an example of classifying fruits as either ‘Apple’ or ‘Orange’ using two features F_1 and F_2 , where F_1 is the color of the fruit, and F_2 is the weight of the fruit. Intuitively, the color of the fruit can potentially simplify the classification process as compared to the weight of the fruit. As a result, if feature F_2 was to be examined first, it would be very probable for feature F_1 to be examined as well to improve the chances of accurate classification. Instead, if F_1 was to be evaluated first, a decision could be made using one feature only. To avoid the computational complexity of evaluating all $K!$ possible feature orderings, we sort features in increasing order of the sum of type I and II errors (considering the

true class as the positive class and all the rest classes as a single negative class), scaled by the cost coefficient of the n th feature to promote low cost features that at the same time are expected to result in few errors. Finally, for F-ETANA, we set $\varepsilon = 10^{-5}$, and $t_{\max} = 10^5$ as the stopping criteria in Algorithm 1.

5.2 Effect of Feature Space Quantization

In Section 5.1, we estimated the conditional probabilities of features given the class using a data binning technique (i.e., $\hat{p}(F_k|T_i) = \frac{N_{k,i+1}}{N_i+V}$). In this subsection, we analyze the effect of the number V of bins on ETANA using four datasets (Lung, Dexter, Madelon, MLL).

In Fig. 4, we plot the variation of the accuracy, the average number of features used for classification, and the training time as a function of V . ETANA’s accuracy and the average number of features used for classification is relatively robust to the number of bins (see Fig. 4(a) and Fig. 4(b)). However, increasing the number of bins from 50 to 100 results in a drop in accuracy for the MLL dataset. Most probably, this is due to overfitting as a result of increasing the resolution of the feature space to a very high value. The linear relationship between training time and the number of bins (see Fig. 4(c)) is due to Eq. (12). Without any loss of generality, in the rest of the experiments we set V to the number of class variables (i.e., N) in the evaluating dataset.

5.3 Accuracy as a Function of the Average Number of Features Used

To study the behavior of ETANA for varying values of feature evaluation cost c , when all features incur same cost (i.e., $c_k = c$), we measured accuracy for constant misclassification costs (i.e., $M_i, j = 1 \forall i \neq j, M_{i,i} = 0, i, j \in \{1, \dots, N\}$) and $c = \{0.1, 0.08, 0.06, 0.04, 0.02, 0.01, 0.001, 0\}$. Different c values result in different number of features and levels of accuracy. Intuitively, using a small portion of the total feature set leads to low accuracy, whereas when the average number of features used increases, the performance improves dramatically. From here onwards, unless specified, we report results for $c = 0.01$.

TABLE 2: Comparison of accuracy. The highest accuracy is bolded and gray-shaded. The second highest value is also gray shaded. Cells are marked with ‘- -’ if the corresponding method was unable to generate results within a cutoff time of 12 days.

Dataset	ETANA	F-ETANA	OFS-Density	OFS-A3M	SAOLA	Fast-OSFS	OSFS	Alpha-Investing
Madelon	0.6233	0.555	0.5117	0.5117	0.5817	0.5417	0.5817	0.6050
Lung C.	0.9673	0.9835	0.9779	0.9557	0.9890	0.9890	0.9724	0.9613
MLL	1.00	1.00	0.9333	0.8667	0.8667	0.8000	0.8000	0.9333
Dexter	0.62	0.62	0.8167	0.7800	0.7800	0.7800	0.7967	0.5000
Car	0.8217	0.8273	0.5854	0.7874	0.7982	0.5869	0.500	0.6429
Lung2	0.8720	0.8818	0.8968	0.8865	0.8817	0.8420	0.8471	0.8820
News20	0.7352	0.6346	--	0.7846	--	--	--	--

TABLE 3: Comparison of average number of features used. Values corresponding to highest and second highest accuracy are bolded and gray-shaded, and gray-shaded accordingly. Cells are marked with ‘- -’ if the corresponding method was unable to generate results within a cutoff time of 12 days.

Dataset	ETANA	F-ETANA	OFS-Density	OFS-A3M	SAOLA	Fast-OSFS	OSFS	Alpha-Investing
Madelon	4.09	211.21	2	2	3	3	3	4
Lung C.	2.78	8.48	25.40	8.20	52	6.8	4.0	4.6
MLL	5.07	10.8	12	9	28	5	3	7
Dexter	6.32	7.04	10	98	21	9	6	1
Car	13.85	289.38	34.8	36.6	41.40	8.4	4.4	24.4
Lung2	13.77	71.66	14.2	18.4	28.2	9.4	5.8	34.4
News20	81.70	4000.6	--	241.8	--	--	--	--

TABLE 4: Comparison of time (in seconds) required for feature selection (F), classification (C), joint feature selection and classification (F+C), and model training (T). Values corresponding to highest and second highest accuracy are bolded and gray-shaded, and gray-shaded accordingly. Cells are marked with ‘- -’ if the corresponding method was unable to generate results within a cutoff time of 12 days.

Dataset	Time	ETANA	F-ETANA	Time	OFS-Density	OFS-A3M	SAOLA	Fast-OSFS	OSFS	Alpha-Investing
Madelon	F+C	0.062	3.678	F	188.85	225.48	0.136	0.199	0.203	0.043
	C			0.024	0.025	0.025	0.025	0.026	0.024	
	T			0.141	0.34	0.423	0.424	0.438	0.429	0.437
Lung Cancer	F+C	0.003	0.014	F	13.455	39.031	4.692	2.644	37.868	1.207
	C	3.680	2.392	C	0.017	0.019	0.017	0.012	0.012	0.012
	T			0.117	0.114	0.118	0.120	0.119	0.121	
MLL	F+C	0.001	0.001	F	1.524	5.122	3.079	1.495	9.354	0.463
	C			0.045	0.023	0.045	0.025	0.025	0.025	0.023
	T			15.376	2.28	0.397	0.401	0.408	0.412	0.409
Dexter	F+C	0.047	0.046	F	98.482	43554	1.006	1.513	3.195	15.663
	C	2.484	2.24	C	0.072	0.080	0.085	0.072	0.066	0.054
	T			0.420	0.423	0.420	0.423	0.427	0.424	
Car	F+C	0.037	0.332	F	7.882	37.205	2.249	1.092	14.144	0.956
	C	1167.5	36.743	C	0.012	0.017	0.017	0.001	0.001	0.017
	T			0.113	0.112	0.117	0.004	0.005	0.117	
Lung2	F+C	0.034	0.071	F	4.214	16.346	1.255	1.681	28.888	0.338
	C	715.03	7.713	C	0.017	0.017	0.017	0.017	0.012	0.017
	T			0.113	0.109	0.115	0.120	0.119	0.116	
News20	F+C	117.61	346.47	F	--	2183	--	--	--	--
	C	3076	429.7	C	--	60.60	--	--	--	--
	T			--	0.586	--	--	--	--	

5.4 Comparison with Online Feature Selection Methods

In this subsection, we compare ETANA and F-ETANA with the following state-of-the-art feature selection methods: OFS-Density [7], OFS-A3M [9], SOAOLA [6], OSFS [5], Fast-OSFS [5], and Alpha-Investing [4]. We use KNN classifier with three neighbours to evaluate a selected feature subset, which has been shown to outperform SVM, CART, and J48 classifiers on the datasets used in [6], [7]. For SAOLA, OSFS, and Fast-OSFS, the parameter α is set to 0.01 [5], [6]. For Alpha-Investing, parameters are set to the values used in [4].

We summarize our observations from Tables 2, 3, 4 by dataset as follows.

Madelon: ETANA achieves the highest accuracy using only

~ 4 features on average. In fact, ETANA achieves an improvement of 3% in accuracy over Alpha-Investing, which has the highest accuracy among all the baselines using the same number of features. At the same time, ETANA is 7.5%, and 67.8% faster in joint feature selection and classification, and model training respectively, compared to Alpha-Investing.

Lung Cancer: SAOLA and Fast-OSFS achieve the highest accuracy using 52, and 6.8 features, respectively, but require 18.7, and 2.4 times more features respectively, compared to ETANA for a difference of 2% in accuracy. Further, ETANA is much faster in joint feature selection and classification compared to SAOLA and Fast-OSFS.

MLL: ETANA and F-ETANA achieve 100% accuracy using 5.07, and 10.8 features on average, respectively. This corre-

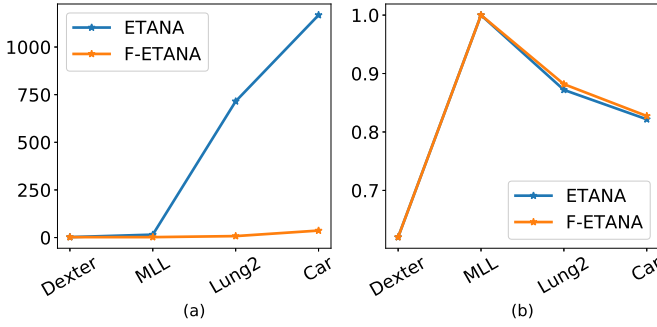


Fig. 5: Comparison of (a) model training time (seconds), and (b) accuracy achieved by F-ETANA and ETANA using Dexter (2 classes), MLL (3 classes), Lung2 (5 classes), and CAR datasets (11 classes).

sponds to an improvement of 7% in accuracy with 57.8%, and 27.6% less of features used compared to OFS-Density and Alpha-Investing, respectively, which achieve the highest accuracy among all the baselines. At the same time, both ETANA and F-ETANA are much faster in joint feature selection and classification compared to OFS-Density and Alpha-Investing.

Dexter: OFS-Density achieves the highest accuracy, but requires 58.2% more features. This results in a significant slowdown for joint feature selection and classification compared to ETANA.

Car: F-ETANA achieves the highest accuracy, however, ETANA is a close second while using only 13.85 features on average. This corresponds to an improvement of 3% and 66.5% in accuracy and average number of features used respectively, while at the same time, leads to a faster runtime compared to SAOLA, the best performing baseline.

Lung2: OFS-Density achieves the highest accuracy with 3.1% more features as compared to ETANA, and much slower runtime.

5.5 Performance Assessment on a High Dimensional Dataset

In this subsection, we discuss the performance of our algorithms, ETANA and F-ETANA, and the state-of-the-art online feature selection methods on the News20 dataset. Experiments on this dataset are conducted using the high performance computing cluster provided by the Information Technology Services at the University of Albany, SUNY. We used one node with 20 Intel(R) Xeon(R) E5-2680 v4 @2.40GHz CPUs with 256 GB memory. Except for SAOLA, the rest of the online feature selection methods were unable to generate results within a cutoff time of 12 days. Although SAOLA achieves the highest accuracy, it requires ~200% more features and is ~20 times slower in joint feature selection and classification compared to ETANA for $c = 0.001$ (see the last row in Tables 2, 3, 4).

5.6 F-ETANA versus ETANA

Thus far we have shown that ETANA outperforms all baselines in terms of accuracy, number of features, and time required for joint feature selection and classification. The limitation of ETANA is in its training time (see Table 4), due to the construction of a $(K + 1) \times d$ matrix which grows

exponentially with the number of classes (see Section 3). F-ETANA drastically reduces the time required for model training as compared to ETANA without sacrificing accuracy (see Fig. 5). At the same time, F-ETANA requires more features per data instance compared to ETANA (see Table 3).

6 CONCLUSION

This paper investigated a new research problem, on-the-fly joint feature selection and classification, which aims to minimize the number of feature evaluations per data instance for fast and accurate classification. Specifically, an optimization problem was defined in terms of the cost of evaluating features and the Bayes risk associated with the classification decision. The optimum solution was derived using dynamic programming and it was shown that the corresponding functions are concave, continuous and piecewise linear. Two algorithms, ETANA and F-ETANA were proposed based on the optimum solution and its properties. The proposed algorithms outperformed state-of-the-art feature selection methods in terms of the average number of features used, classification accuracy, and the time required for on-the-fly joint feature selection and classification. Furthermore, F-ETANA resulted in a drastic reduction in model training time compared to ETANA. As a part of our future work, we plan to exploit feature dependencies, which may improve performance even more.

APPENDIX A

A.1 Proof of Lemma 1

We start from the definition of the *a posteriori probability* vector, i.e.:

$$\pi_k \triangleq [\pi_k^1, \pi_k^2, \dots, \pi_k^N]^T,$$

and consider any element in this vector, i.e., π_k^i . Specifically, we use Bayes' rule and the law of total probability to get the following result:

$$\begin{aligned} \pi_k^i &= P(T_i | F_1, \dots, F_k) \\ &= \frac{P(F_1, \dots, F_k | T_i) P(T_i)}{P(F_1, \dots, F_k)} \end{aligned} \quad (20)$$

$$\begin{aligned} &= \frac{P(F_1, \dots, F_k | T_i) P(T_i)}{\sum_{j=1}^N P(F_1, \dots, F_k | T_j) P(T_j)} \\ &= \frac{P(F_1, \dots, F_k | T_i) P(T_i)}{\sum_{j=1}^N P(F_1, \dots, F_k | T_j) P(T_j)}. \end{aligned} \quad (21)$$

Note that we can further simplify Eq. (21) by exploiting the conditional independence of the features in set F given the class variable T as follows:

$$\begin{aligned} \pi_k^i &= \frac{P(T_i) \prod_{n=1}^k P(F_n | T_i)}{\sum_{j=1}^N P(T_j) \prod_{n=1}^k P(F_n | T_j)} \\ &= \frac{p_i \prod_{n=1}^k P(F_n | T_i)}{\sum_{j=1}^N p_j \prod_{n=1}^k P(F_n | T_j)}. \end{aligned} \quad (22)$$

Similarly, π_{k-1}^i will take the following form:

$$\pi_{k-1}^i = \frac{p_i \prod_{n=1}^{k-1} P(F_n | T_i)}{\sum_{j=1}^N p_j \prod_{n=1}^{k-1} P(F_n | T_j)}. \quad (23)$$

We can now rewrite π_k^i in Eq. (22) in terms of π_{k-1}^i in Eq. (23) as follows:

$$\begin{aligned}\pi_k^i &= \frac{p_i \prod_{n=1}^k P(F_n|T_i)}{\sum_{j=1}^N p_j \prod_{n=1}^k P(F_n|T_j)} \\ &= \frac{P(F_k|T_i)(p_i \prod_{n=1}^{k-1} P(F_n|T_i))}{\sum_{j=1}^N p_j \prod_{n=1}^k P(F_n|T_j)} \\ &= \frac{P(F_k|T_i)(\pi_{k-1}^i \sum_{j=1}^N p_j \prod_{n=1}^{k-1} P(F_n|T_j))}{\sum_{j=1}^N p_j \prod_{n=1}^k P(F_n|T_j)} \\ &= \frac{P(F_k|T_i)\pi_{k-1}^i}{\frac{\sum_{j=1}^N p_j \prod_{n=1}^k P(F_n|T_j)}{\sum_{j=1}^N p_j \prod_{n=1}^{k-1} P(F_n|T_j)}} \\ &= \frac{P(F_k|T_i)\pi_{k-1}^i}{\sum_{j=1}^N P(F_k|T_j)\pi_{k-1}^j}.\end{aligned}\quad (24)$$

Finally, using the above result, the *a posteriori* probability vector takes the following form:

$$\begin{aligned}\pi_k &= [\pi_k^1, \pi_k^2, \dots, \pi_k^N]^T \\ &= \frac{\text{diag}([P(F_k|T_1), \dots, P(F_k|T_N)])[\pi_{k-1}^1, \dots, \pi_{k-1}^N]^T}{[P(F_k|T_1), \dots, P(F_k|T_N)][\pi_{k-1}^1, \dots, \pi_{k-1}^N]^T} \\ &= \frac{\text{diag}([P(F_k|T_1), \dots, P(F_k|T_N)])\pi_{k-1}}{[P(F_k|T_1), \dots, P(F_k|T_N)]\pi_{k-1}} \\ &= \frac{\text{diag}(\Delta_k(F_k))\pi_{k-1}}{\Delta_k^T(F_k)\pi_{k-1}},\end{aligned}\quad (25)$$

where $\Delta_k(F_k) \triangleq [P(F_k|T_1), P(F_k|T_2), \dots, P(F_k|T_N)]^T$, $\text{diag}(A)$ denotes a diagonal matrix with diagonal elements being the elements in vector A , and $\pi_0 \triangleq [p_1, p_2, \dots, p_N]^T$.

A.2 Proof of Lemma 2

Using the law of total probability, we can write the probability $P(D_R = j, T_i)$ as follows:

$$\begin{aligned}P(D_R = j, T_i) &= \sum_{k=1}^K P(R = k, D_k = j, T_i) \\ &= \sum_{k=1}^K P(T_i)P(R = k, D_k = j|T_i).\end{aligned}\quad (26)$$

Using the fact that the event $\{R = k, D_k = j\}$ depends only on the set $\{F_1, F_2, \dots, F_k\}$, and by the definition $P(R = k, D_k = j) = E\{\mathbb{1}_{\{R=k\}}\mathbb{1}_{\{D_k=j\}}\}$, Eq. (26) can be written as follows:

$$\begin{aligned}P(D_R = j, T_i) &= \sum_{k=1}^K \sum_{F_1, F_2, \dots, F_k} \mathbb{1}_{\{R=k\}}\mathbb{1}_{\{D_k=j\}} \\ &\quad \times P(T_i)P(F_1, \dots, F_k|T_i).\end{aligned}\quad (27)$$

Then, using the result in Eq. (20), we can incorporate π_k^i in Eq. (27) as follows:

$$\begin{aligned}P(D_R = j, T_i) &= \sum_{k=1}^K \sum_{F_1, F_2, \dots, F_k} \mathbb{1}_{\{R=k\}}\mathbb{1}_{\{D_k=j\}} \\ &\quad \times P(F_1, \dots, F_k)\pi_k^i.\end{aligned}\quad (28)$$

Further, from the definition of the expectation operator (i.e., if a random variable Y has set D of possible values and probability mass function $P(Y)$, then the expected value

$\mathbb{E}\{H(Y)\}$ of any function $H(Y)$ equals $\sum_{Y \in D} P(Y)H(Y)$), Eq. (28) can be rewritten as follows:

$$P(D_R = j, T_i) = \sum_{k=1}^K \mathbb{E}\{\mathbb{1}_{\{R=k\}}\mathbb{1}_{\{D_k=j\}}\pi_k^i\}.\quad (29)$$

By the *linearity of expectation* in Eq. (29), we get:

$$P(D_R = j, T_i) = \mathbb{E}\left\{\sum_{k=1}^K \mathbb{1}_{\{R=k\}}\mathbb{1}_{\{D_k=j\}}\pi_k^i\right\}.\quad (30)$$

Finally, using the fact that $x_R = \sum_{k=0}^K x_k \mathbb{1}_{\{R=k\}}$, Eq. (30) will end up in the desired form as shown below:

$$P(D_R = j, T_i) = \mathbb{E}\{\pi_R^i \mathbb{1}_{\{D_R=j\}}\}.\quad (31)$$

A.3 Proof of Theorem 1

At any stopping time R , the optimum decision D_R takes only one out of N possibilities such that the misclassification cost is minimum. In the process of finding this optimum D_R , it is important to note that $\sum_{j=1}^N \mathbb{1}_{\{D_R=j\}} = 1$, where $\mathbb{1}_A$ is the indicator function for event A (i.e., $\mathbb{1}_A = 1$ when A occurs, and $\mathbb{1}_A = 0$ otherwise), which implies that only one of the terms in the sum becomes 1, while the remaining terms are equal to zero. We note that:

$$M_j^T \pi_R \geq g(\pi_R), \quad \forall j \in \{1, 2, \dots, N\},\quad (32)$$

where $g(\pi_R) \triangleq \min_{1 \leq j \leq N} [M_j^T \pi_R]$. Then, using the fact that $\mathbb{1}_{\{D_R=j\}}$ is non-negative, we get the following result:

$$\begin{aligned}\sum_{j=1}^N (M_j^T \pi_R) \mathbb{1}_{\{D_R=j\}} &\geq g(\pi_R) \sum_{j=1}^N \mathbb{1}_{\{D_R=j\}} \\ &= g(\pi_R).\end{aligned}\quad (33)$$

We underscore that the lower bound $g(\pi_R)$ derived above is independent of the decision D_R . Thus, it is obvious that this lower bound can be achieved only by the rule defined in Eq. (8), which is therefore the optimum decision for a given stopping time R .

A.4 Proof of Theorem 2

At the end of the K th stage, assuming that all the features have been examined, the only remaining expected cost is the optimum misclassification cost of selecting among N decision choices at stage $k = K$, which is $\bar{J}_K(\pi_K) = g(\pi_K)$ (see Theorem 1).

Then, consider any intermediate stage $k = 0, 1, \dots, K-1$. Being at stage k , with the available information π_k , the optimum strategy has to choose between, either to terminate the feature evaluation process and incur cost $g(\pi_k)$, which is the optimum misclassification cost of selecting among N decision choices (see Theorem 1), or continue and incur cost of c_{k+1} to evaluate feature F_{k+1} and an additional cost $\bar{J}_{k+1}(\pi_{k+1})$ to continue optimally. Thus, the total cost of continuing optimally (referred to as *optimum cost-to-go* [40]) is $c_{k+1} + \bar{J}_{k+1}(\pi_{k+1})$. It is important to note that at stage k , we do not know the outcome of examining feature F_{k+1} . Thus, we need to consider the expected *optimum cost-to-go*, which is equal to $c_{k+1} + \mathbb{E}\{\bar{J}_{k+1}(\pi_{k+1})|\pi_k\}$. Using Lemma 1 to express π_{k+1} in terms of π_k , and by the definition of the expectation operator (i.e., if a random variable Y has set

D of possible values and probability mass function $P(Y)$, then the expected value $\mathbb{E}\{H(Y)\}$ of any function $H(Y)$ equals to $\sum_{Y \in D} P(Y)H(Y)$, we get the *optimum cost-to-go* $\bar{C}_{k+1}(\pi_k)$:

$$\begin{aligned} \bar{C}_{k+1}(\pi_k) &\triangleq c_{k+1} + \mathbb{E}\{\bar{J}_{k+1}(\pi_{k+1})|\pi_k\} \\ &= c_{k+1} + \sum_{F_{k+1}} P(F_{k+1}|F_1, F_2, \dots, F_k) \\ &\quad \times \bar{J}_{k+1}\left(\frac{\text{diag}(\Delta_{k+1}(F_{k+1}))\pi_k}{\Delta_{k+1}^T(F_{k+1})\pi_k}\right). \end{aligned} \quad (34)$$

Let us simplify the term $P(F_{k+1}|F_1, F_2, \dots, F_k)$ separately. Specifically, using Bayes' rule and the law of total probability, we observe that:

$$\begin{aligned} P(F_{k+1}|F_1, \dots, F_k) &= \frac{P(F_1, \dots, F_{k+1})}{P(F_1, \dots, F_k)} \\ &= \frac{\sum_{T_j=1}^N P(F_1, \dots, F_{k+1}, T_j)}{\sum_{T_j=1}^N P(F_1, \dots, F_k, T_j)} \\ &= \frac{\sum_{T_j=1}^N P(F_1, \dots, F_{k+1}|T_j)P(T_j)}{\sum_{T_j=1}^N P(F_1, \dots, F_k|T_j)P(T_j)}. \end{aligned} \quad (35)$$

Note that we can further simplify Eq. (35) by exploiting the fact that the random variables F_k are independent under each class T_j as follows:

$$\begin{aligned} P(F_{k+1}|F_1, \dots, F_k) &= \frac{\sum_{T_j=1}^N P(T_j) \prod_{n=1}^{k+1} P(F_n|T_j)}{\sum_{T_j=1}^N P(T_j) \prod_{n=1}^k P(F_n|T_j)} \\ &= \frac{\sum_{T_j=1}^N \left(p_j \prod_{n=1}^k P(F_n|T_j) \right) P(F_{k+1}|T_j)}{\sum_{T_j=1}^N p_j \prod_{n=1}^k P(F_n|T_j)}. \end{aligned} \quad (36)$$

Using the result in Eq. (22), we can simplify Eq. (36) as follows:

$$\begin{aligned} P(F_{k+1}|F_1, \dots, F_k) &= \sum_{j=1}^N \pi_k^j P(F_{k+1}|T_j) \\ &= \Delta_{k+1}^T(F_{k+1})\pi_k. \end{aligned} \quad (37)$$

Finally, substituting Eq. (37) in Eq. (34), we get the desired result:

$$\begin{aligned} \bar{C}_{k+1}(\pi_k) &= c_{k+1} + \sum_{F_{k+1}} \Delta_{k+1}^T(F_{k+1})\pi_k \\ &\quad \times \bar{J}_{k+1}\left(\frac{\text{diag}(\Delta_{k+1}(F_{k+1}))\pi_k}{\Delta_{k+1}^T(F_{k+1})\pi_k}\right). \end{aligned} \quad (38)$$

APPENDIX B

B.1 Proof of Lemma 3

Let us consider the definition of $g(\varpi)$:

$$g(\varpi) \triangleq \min_{1 \leq j \leq N} [M_j^T \varpi], \varpi \in [0, 1]^N.$$

The term $M_j^T \varpi$ is linear with respect to ϖ , and since the minimum of linear functions is a concave, piecewise linear function, we conclude that $g(\varpi)$ is a concave, piecewise linear function as well. Concavity also assures the continuity of this function. Finally, minimization over finite N hyperplanes guarantees that the function $g(\varpi)$ is made up of at most N hyperplanes.

B.2 Proof of Lemma 4

First, let us consider the function $\bar{J}_{K-1}(\varpi)$ given by:

$$\begin{aligned} \bar{J}_{K-1}(\varpi) &= \min \left[g(\varpi), c_K + \sum_{F_K} \Delta_K^T(F_K)\varpi \right. \\ &\quad \left. \times \bar{J}_K\left(\frac{\text{diag}(\Delta_K(F_K))\varpi}{\Delta_K^T(F_K)\varpi}\right) \right]. \end{aligned} \quad (39)$$

Using the fact that $\bar{J}_K(\pi_K) = g(\pi_K)$, we can rewrite Eq. (39) as follows:

$$\begin{aligned} \bar{J}_{K-1}(\varpi) &= \min \left[g(\varpi), c_K + \sum_{F_K} \Delta_K^T(F_K)\varpi \right. \\ &\quad \left. \times g\left(\frac{\text{diag}(\Delta_K(F_K))\varpi}{\Delta_K^T(F_K)\varpi}\right) \right]. \end{aligned} \quad (40)$$

We focus our attention on the following function inside the summation of Eq. (40):

$$Q(\varpi) \triangleq \Delta_K^T(F_K)\varpi g\left(\frac{\text{diag}(\Delta_K(F_K))\varpi}{\Delta_K^T(F_K)\varpi}\right). \quad (41)$$

Using the definition of $g(\varpi)$ in Eq. (13), we can rewrite Eq. (41) as follows:

$$\begin{aligned} Q(\varpi) &= \Delta_K^T(F_K)\varpi \min_{1 \leq j \leq N} \left[M_j^T \frac{\text{diag}(\Delta_K(F_K))\varpi}{\Delta_K^T(F_K)\varpi} \right] \\ &= \min_{1 \leq j \leq N} \left[\Delta_K^T(F_K)\varpi M_j^T \frac{\text{diag}(\Delta_K(F_K))\varpi}{\Delta_K^T(F_K)\varpi} \right] \\ &= \min_{1 \leq j \leq N} \left[M_j^T \text{diag}(\Delta_K(F_K))\varpi \right]. \end{aligned} \quad (42)$$

Note that the term $M_j^T \text{diag}(\Delta_K(F_K))\varpi$ is linear with respect to ϖ . Using the fact that the minimum of linear functions is a concave, piecewise linear function, implies that $Q(\varpi)$ is a concave, piecewise linear function. Furthermore, we recall: i) the non-negative sum of concave/piecewise linear functions is also a concave/piecewise linear function, and ii) the minimum of two concave/piecewise linear functions is also a concave/piecewise linear function. Based on these two facts, and the fact that $\Delta_K(F_K)$ is a probability vector which is non-negative, we conclude that the function $\bar{J}_{K-1}(\varpi)$ in Eq. (39) is concave and piecewise linear. Concavity also assures the continuity of this function.

Then, let us consider the function $\bar{J}_{K-2}(\varpi)$ given by:

$$\begin{aligned} \bar{J}_{K-2}(\varpi) &= \min \left[g(\varpi), c_{K-1} + \sum_{F_{K-1}} \Delta_{K-1}^T(F_{K-1})\varpi \right. \\ &\quad \left. \times \bar{J}_{K-1}\left(\frac{\text{diag}(\Delta_{K-1}(F_{K-1}))\varpi}{\Delta_{K-1}^T(F_{K-1})\varpi}\right) \right]. \end{aligned} \quad (43)$$

We have already proved that the functions $\bar{J}_{K-1}(\varpi)$ and $g(\varpi)$ are concave and piecewise linear. Using the facts that i) the non-negative sum of concave/piecewise linear functions is also a concave/piecewise linear function, and ii) the minimum of two concave/piecewise linear functions is also a concave/piecewise linear function, we conclude that the function $\bar{J}_{K-2}(\varpi)$ is also concave and piecewise linear. Concavity also assures the continuity of this function. Using similar arguments, the concavity, the continuity and the piecewise linearity of functions $\bar{J}_k(\varpi)$, $n = 0, \dots, K-3$,

can also be guaranteed.

B.3 Proof of Theorem 3

Let us start the proof by showing that all N corners of the $N - 1$ dimensional unit simplex always correspond to stopping irrespective of the stage. In other words, when $\varpi = e_i$, $g(\varpi) < \bar{C}_{k+1}(\varpi)$, for all $k = 0, \dots, K - 1$, where e_i denotes the column vector with a 1 in the i th coordinate and 0's elsewhere. At stage $k = K - 1$, we have that:

$$\begin{aligned}
\bar{C}_K(\varpi) &= c_K + \sum_{F_K} \Delta_K^T(F_K) e_i \bar{J}_K \left(\frac{\text{diag}(\Delta_K(F_K)) e_i}{\Delta_K^T(F_K) e_i} \right) \\
&= c_K + \sum_{F_K} \Delta_K^T(F_K) e_i g \left(\frac{\text{diag}(\Delta_K(F_K)) e_i}{\Delta_K^T(F_K) e_i} \right) \\
&= c_K + \sum_{F_K} P(F_K|T_i) g \left(\frac{P(F_K|T_i) e_i}{P(F_K|T_i)} \right) \\
&= c_K + g(e_i) \sum_{F_K} P(F_K|T_i) \\
&= c_K + g(e_i) \\
&> g(e_i), \tag{44}
\end{aligned}$$

where the last inequality holds since $c_K > 0$. From Eq. (39), we see that $\bar{J}_{K-1}(e_i) = g(e_i)$. Then, let us consider the case $k = K - 2$ as follows:

$$\begin{aligned}
\bar{C}_{K-1}(\varpi) &= c_{K-1} + \sum_{F_{K-1}} \Delta_{K-1}^T(F_{K-1}) e_i \\
&\quad \times \bar{J}_{K-1} \left(\frac{\text{diag}(\Delta_{K-1}(F_{K-1})) e_i}{\Delta_{K-1}^T(F_{K-1}) e_i} \right) \\
&= c_{K-1} + \sum_{F_{K-1}} P(F_{K-1}|T_i) \bar{J}_{K-1} \left(\frac{P(F_{K-1}|T_i) e_i}{P(F_{K-1}|T_i)} \right) \\
&= c_{K-1} + \bar{J}_{K-1}(e_i) \sum_{F_{K-1}} P(F_{K-1}|T_i) \\
&= c_{K-1} + g(e_i) \sum_{F_{K-1}} P(F_{K-1}|T_i) \\
&= c_{K-1} + g(e_i) \\
&> g(e_i), \tag{45}
\end{aligned}$$

where the last inequality holds since $c_{K-1} > 0$. Using similar arguments, the latter result can be proven for all $k = 0, \dots, K - 3$. The rest of the proof is very intuitive. Using the facts: (i) the functions $\bar{C}_{k+1}(\varpi)$ are concave (see the proof of Lemma 4), and (ii) the simplex corners always correspond to stopping, we see that the hyperplanes of $g(\varpi)$ connected to the N corners of the unit simplex can have only one intersection with each $\bar{C}_{k+1}(\varpi)$. Finally, using the fact that $g(\varpi)$ is made up of at most N hyperplanes (see Lemma 3), we conclude that at every stage k , there are at most N threshold curves which split up the probability space of ϖ (i.e., the $N - 1$ dimensional unit simplex) into areas that correspond to either continuing or stopping.

ACKNOWLEDGMENTS

This material is based upon work supported by the National Science Foundation under Grant No. ECCS-1737443.

REFERENCES

- [1] I. Guyon and A. Elisseeff, "An introduction to variable and feature selection," *Journal of machine learning research*, vol. 3, no. Mar, pp. 1157–1182, 2003.
- [2] H. Liu and L. Yu, "Toward integrating feature selection algorithms for classification and clustering," *IEEE Transactions on Knowledge & Data Engineering*, no. 4, pp. 491–502, 2005.
- [3] S. Perkins and J. Theiler, "Online feature selection using grafting," in *Proceedings of the 20th International Conference on Machine Learning (ICML-03)*, 2003, pp. 592–599.
- [4] J. Zhou, D. Foster, R. Stine, and L. Ungar, "Streaming feature selection using alpha-investing," in *Proceedings of the eleventh ACM SIGKDD international conference on Knowledge discovery in data mining*. ACM, 2005, pp. 384–393.
- [5] X. Wu, K. Yu, W. Ding, H. Wang, and X. Zhu, "Online feature selection with streaming features," *IEEE transactions on pattern analysis and machine intelligence*, vol. 35, no. 5, pp. 1178–1192, 2012.
- [6] K. Yu, X. Wu, W. Ding, and J. Pei, "Towards scalable and accurate online feature selection for big data," in *2014 IEEE International Conference on Data Mining*. IEEE, 2014, pp. 660–669.
- [7] P. Zhou, X. Hu, P. Li, and X. Wu, "Ofs-density: A novel online streaming feature selection method," *Pattern Recognition*, vol. 86, pp. 48–61, 2019.
- [8] S. Eskandari and M. M. Javidi, "Online streaming feature selection using rough sets," *International Journal of Approximate Reasoning*, vol. 69, pp. 35–57, 2016.
- [9] P. Zhou, X. Hu, P. Li, and X. Wu, "Online streaming feature selection using adapted neighborhood rough set," *Information Sciences*, vol. 481, pp. 258–279, 2019.
- [10] M. M. Javidi and S. Eskandari, "Online streaming feature selection: a minimum redundancy, maximum significance approach," *Pattern Analysis and Applications*, vol. 22, no. 3, pp. 949–963, 2019.
- [11] S. C. Hoi, J. Wang, P. Zhao, and R. Jin, "Online feature selection for mining big data," in *Proceedings of the 1st international workshop on big data, streams and heterogeneous source mining: Algorithms, systems, programming models and applications*. ACM, 2012, pp. 93–100.
- [12] J. Wang, P. Zhao, S. C. H. Hoi, and R. Jin, "Online feature selection and its applications," *IEEE Transactions on Knowledge and Data Engineering*, vol. 26, no. 3, pp. 698–710, March 2014.
- [13] Y. Wu, S. C. Hoi, T. Mei, and N. Yu, "Large-scale online feature selection for ultra-high dimensional sparse data," *ACM Transactions on Knowledge Discovery from Data (TKDD)*, vol. 11, no. 4, p. 48, 2017.
- [14] J. Li, K. Cheng, S. Wang, F. Morstatter, R. P. Trevino, J. Tang, and H. Liu, "Feature selection: A data perspective," *ACM Computing Surveys (CSUR)*, vol. 50, no. 6, p. 94, 2018.
- [15] J. Wang, J.-M. Wei, Z. Yang, and S.-Q. Wang, "Feature selection by maximizing independent classification information," *IEEE Transactions on Knowledge and Data Engineering*, vol. 29, no. 4, pp. 828–841, 2017.
- [16] Z. Zhang and K. K. Parhi, "Muse: Minimum uncertainty and sample elimination based binary feature selection," *IEEE Transactions on Knowledge and Data Engineering*, 2018.
- [17] G. Chandrashekar and F. Sahin, "A survey on feature selection methods," *Computers & Electrical Engineering*, vol. 40, no. 1, pp. 16–28, 2014.
- [18] Y. Saeyns, I. Inza, and P. Larrañaga, "A review of feature selection techniques in bioinformatics," *bioinformatics*, vol. 23, no. 19, pp. 2507–2517, 2007.
- [19] X. Hu, P. Zhou, P. Li, J. Wang, and X. Wu, "A survey on online feature selection with streaming features," *Frontiers of Computer Science*, vol. 12, no. 3, pp. 479–493, 2018.
- [20] N. AlNuaimi, M. M. Masud, M. A. Serhani, and N. Zaki, "Streaming feature selection algorithms for big data: A survey," *Applied Computing and Informatics*, 2019.
- [21] V. Bolón-Canedo, I. Porto-Díaz, N. Sánchez-Marño, and A. Alonso-Betanzos, "A framework for cost-based feature selection," *Pattern Recognition*, vol. 47, no. 7, pp. 2481–2489, 2014.
- [22] W. Shu and H. Shen, "Multi-criteria feature selection on cost-sensitive data with missing values," *Pattern Recognition*, vol. 51, pp. 268–280, 2016.
- [23] F. Rosenblatt, "The perceptron: a probabilistic model for information storage and organization in the brain." *Psychological review*, vol. 65, no. 6, p. 386, 1958.
- [24] A. B. Novikoff, "On convergence proofs for perceptrons," STANFORD RESEARCH INST MENLO PARK CA, Tech. Rep., 1963.

- [25] K. Crammer, O. Dekel, J. Keshet, S. Shalev-Shwartz, and Y. Singer, "Online passive-aggressive algorithms," *Journal of Machine Learning Research*, vol. 7, no. Mar, pp. 551–585, 2006.
- [26] J. Duchi, E. Hazan, and Y. Singer, "Adaptive subgradient methods for online learning and stochastic optimization," *Journal of Machine Learning Research*, vol. 12, no. Jul, pp. 2121–2159, 2011.
- [27] T. van Erven and W. M. Koolen, "Metagrad: Multiple learning rates in online learning," in *Advances in Neural Information Processing Systems*, 2016, pp. 3666–3674.
- [28] H. Luo, A. Agarwal, N. Cesa-Bianchi, and J. Langford, "Efficient second order online learning by sketching," in *Advances in Neural Information Processing Systems*, 2016, pp. 902–910.
- [29] L. Zhang, S. Lu, and Z.-H. Zhou, "Adaptive online learning in dynamic environments," in *Advances in Neural Information Processing Systems*, 2018, pp. 1323–1333.
- [30] Y. Li and P. M. Long, "The relaxed online maximum margin algorithm," *Machine Learning*, vol. 46, no. 1, pp. 361–387, 2002.
- [31] J. Wang, P. Zhao, and S. C. Hoi, "Cost-sensitive online classification," *IEEE Transactions on Knowledge and Data Engineering*, vol. 26, no. 10, pp. 2425–2438, 2013.
- [32] P. Zhao, Y. Zhang, M. Wu, S. C. Hoi, M. Tan, and J. Huang, "Adaptive cost-sensitive online classification," *IEEE Transactions on Knowledge and Data Engineering*, vol. 31, no. 2, pp. 214–228, 2018.
- [33] S. C. Hoi, D. Sahoo, J. Lu, and P. Zhao, "Online learning: A comprehensive survey," *arXiv preprint arXiv:1802.02871*, 2018.
- [34] C. Zhang, H. Wei, J. Zhao, T. Liu, T. Zhu, and K. Zhang, "Short-term wind speed forecasting using empirical mode decomposition and feature selection," *Renewable Energy*, vol. 96, pp. 727–737, 2016.
- [35] S. Yang, "On feature selection for traffic congestion prediction," *Transportation Research Part C: Emerging Technologies*, vol. 26, pp. 160–169, 2013.
- [36] M.-C. Lee, "Using support vector machine with a hybrid feature selection method to the stock trend prediction," *Expert Systems with Applications*, vol. 36, no. 8, pp. 10 896–10 904, 2009.
- [37] C. Ding and H. Peng, "Minimum redundancy feature selection from microarray gene expression data," *Journal of bioinformatics and computational biology*, vol. 3, no. 02, pp. 185–205, 2005.
- [38] J.-H. Seo, Y. H. Lee, and Y.-H. Kim, "Feature selection for very short-term heavy rainfall prediction using evolutionary computation," *Advances in Meteorology*, vol. 2014, 2014.
- [39] A. N. Shiryaev, *Optimal Stopping Rules*. Springer Science & Business Media, 2007, vol. 8.
- [40] D. P. Bertsekas, *Dynamic Programming and Optimal Control*. Athena Scientific, 2005, vol. 1.
- [41] K. Yang, Z. Cai, J. Li, and G. Lin, "A stable gene selection in microarray data analysis," *BMC bioinformatics*, vol. 7, no. 1, p. 228, 2006.
- [42] J. C. Spall, *Introduction to stochastic search and optimization: estimation, simulation, and control*. John Wiley & Sons, 2005, vol. 65.
- [43] G. C. Pflug, *Optimization of stochastic models: the interface between simulation and optimization*. Springer Science & Business Media, 2012, vol. 373.
- [44] "Colpnet: Feature Selection Challenge," [Online]. Available: <http://colpnet.com/isabelle/Projects/NIPS2003/>.
- [45] "LIBSVM data sets," [Online]. Available: <https://www.csie.ntu.edu.tw/~cjlin/libsvmtools/datasets/>.



Yasitha Warahena Liyanage received the B.S. degree in electrical and electronic engineering from the University of Peradeniya, Sri Lanka, in 2016. Currently, he is working toward the Ph.D. degree in electrical and computer engineering at the University at Albany, SUNY. His research interests include quickest change detection, optimal stopping theory and machine learning.



Daphney-Stavroula Zois received the B.S. degree in computer engineering and informatics from the University of Patras, Patras, Greece, and the M.S. and Ph.D. degrees in electrical engineering from the University of Southern California, Los Angeles, CA, USA. Previous appointments include the University of Illinois, Urbana-Champaign, IL, USA. She is an Assistant Professor in the Department of Electrical and Computer Engineering, University at Albany, State University of New York, Albany, NY, USA. She

received the Viterbi Dean's and Myronis Graduate Fellowships. She has served and is serving as Co-Chair, TPC member or reviewer in international conferences and journals, such as GlobalSIP, Globecom, and ICASSP, and IEEE Transactions on Signal Processing. Her research interests include decision making under uncertainty, machine learning, detection & estimation theory, intelligent systems design, and signal processing.



Charalampos Chelms is an Assistant Professor in Computer Science at the University at Albany, State University of New York, and the director of the Intelligent Big Data Analytics, Applications, and Systems (IDIAS) Lab, focusing on problems involving big, often networked, data. He has served and is serving as Co-Chair, TPC member or reviewer in numerous international conferences and journals such as ASONAM, SocInfo, and ICWSM. Currently, he serves as Associate Editor of the Journal of Parallel and

Distributed Systems, and served as Guest Editor for the Encyclopedia of Social Network Analysis and Mining. He received the B.S. degree in computer engineering and informatics from the University of Patras, Greece in 2007, and the M.S. and Ph.D. degrees in computer science from the University of Southern California in 2010 and 2013, respectively.